Hidenori Ohnishi, MD, PhD[a]
Rie Miyata, MD, PhD[b]
Tomonori Suzuki, MD[b]
Touichiro Nose, MD[b]
Kazuo Kubota, MD[a]
Zenichiro Kato, MD, PhD[a]
Hideo Kaneko, MD, PhD[a,c]
Naomi Kondo, MD, PhD[a]

From [a]the Department of Pediatrics, Graduate School of Medicine, Gifu University, Gifu, Japan; [b]the Department of Pediatrics, Tokyo-kita Social Insurance Hospital, Tokyo, Japan; [c]the Department of Clinical Research, Nagara Medical Center, Gifu, Japan E-mail: ohnishih@gifu-u.ac.jp.

This study was supported by the Ministry of Health, Labour and Welfare of Japan.
Disclosure of potential conflict of interest: The authors declare that they have no relevant conflicts of interest.

REFERENCES

1. Kawai T, Akira S. The role of pattern-recognition receptors in innate immunity: update on Toll-like receptors. Nat Immunol 2010;11:373-84.
2. Picard C, von Bernuth H, Ghandil P, Chrabieh M, Levy O, Arkwright PD, et al. Clinical features and outcome of patients with IRAK-4 and MyD88 deficiency. Medicine 2010;89:403-25.
3. Doffinger R, Smahi A, Bessia C, Geissmann F, Feinberg J, Durandy A, et al. X-linked anhidrotic ectodermal dysplasia with immunodeficiency is caused by impaired NF-kappaB signaling. Nat Genet 2001;27:277-85.
4. Courtois G, Smahi A, Reichenbach J, Doffinger R, Cancrini C, Bonnet M, et al. A hypermorphic IkappaBalpha mutation is associated with autosomal dominant anhidrotic ectodermal dysplasia and T cell immunodeficiency. J Clin Investig 2003;112:1108-15.
5. Takada H, Yoshikawa H, Imaizumi M, Kitamura T, Takeyama J, Kumaki S, et al. Delayed separation of the umbilical cord in two siblings with interleukin-1 receptor-associated kinase 4 deficiency: rapid screening by flow cytometer. J Pediatr 2006;148:546-8.
6. Lopez-Granados E, Keenan JE, Kinney MC, Leo H, Jain N, Ma CA, et al. A novel mutation in NFKBIA/IKBA results in a degradation-resistant N-truncated protein and is associated with ectodermal dysplasia with immunodeficiency. Hum Mut 2008;29:861-8.
7. McDonald DR, Mooster JL, Reddy M, Bawle E, Secord E, Geha RS. Heterozygous N-terminal deletion of IkappaBalpha results in functional nuclear factor kappaB haploinsufficiency, ectodermal dysplasia, and immune deficiency. J Allergy Clin Immunol 2007;120:900-7.
8. Filipe-Santos O, Bustamante J, Haverkamp MH, Vinolo E, Ku CL, Puel A, et al. X-linked susceptibility to mycobacteria is caused by mutations in NEMO impairing CD40-dependent IL-12 production. J Exp Med 2006;203:1745-59.

doi:10.1016/j.jaci.2011.09.042

J Clin Immunol
DOI 10.1007/s10875-011-9629-0

Characterization of *NLRP3* Variants in Japanese Cryopyrin-Associated Periodic Syndrome Patients

Hidenori Ohnishi · Takahide Teramoto · Hiroaki Iwata · Zenichiro Kato · Takeshi Kimura · Kazuo Kubota · Ryuta Nishikomori · Hideo Kaneko · Mariko Seishima · Naomi Kondo

Received: 5 August 2011 / Accepted: 1 December 2011

Abstract The etiology of cryopyrin-associated periodic syndrome (CAPS) is caused by germline gene mutations in NOD-like receptor family, pryin domain containing 3 (*NLRP3*)/cold-induced autoinflammatory syndrome 1 (*CIAS1*). CAPS includes diseases with various severities. The aim of this study was to characterize patients according to the disease severity of CAPS. Five Japanese patients with four kinds of gene variations in *NLRP3* were found and diagnosed as CAPS or juvenile idiopathic arthritis. Two mutations in *NLRP3*, Y563N and E688K, found in CAPS patients exhibit significant positive activities in the nuclear factor-κB reporter gene assay. Increased serum interleukin (IL)-18 levels were only observed in severe cases of CAPS. In mild cases of CAPS, the serum IL-18 levels were not increased, although lipopolysaccharide- or hypothermia-enhanced IL-1β and IL-18 production levels by their peripheral blood mononuclear cells were detectable. This series of case reports suggests that a combination of in vitro assays could be a useful tool for the diagnosis and characterization of the disease severity of CAPS.

Keywords Autoinflammatory disease · cryopyrin · familial cold autoinflammatory syndrome · interleukin-18 · *NLRP3*

Abbreviations

CAPS	Cryopyrin-associated periodic syndrome
CIAS1	Cold-induced autoinflammatory syndrome 1
CINCA	Chronic infantile neurologic cutaneous and articular
CRP	C-reactive protein
FCAS	Familial cold autoinflammatory syndrome
HEK	Human embryonic kidney
IL	Interleukin
JIA	Juvenile idiopathic arthritis
LPS	Lipopolysaccharide
MWS	Muckle–Wells syndrome
NLRP3	NOD-like receptor family, pryin domain containing 3
NF-κB	Nuclear factor-κB
NOMID	Neonatal-onset multisystem inflammatory disease
PBMCs	Peripheral blood mononuclear cells
TNF	Tumor necrosis factor

Introduction

Cryopyrin-associated periodic syndrome (CAPS) is an autoinflammatory syndrome [1] caused by germline gene mutations in NOD-like receptor family, pryin domain containing 3 (*NLRP3*)/cold-induced autoinflammatory syndrome 1 (*CIAS1*) [2–4]. The diagnosis of CAPS is based on its

H. Ohnishi (✉) · T. Teramoto · Z. Kato · T. Kimura · K. Kubota · H. Kaneko · N. Kondo
Department of Pediatrics, Graduate School of Medicine,
Gifu University,
1-1 Yanagido,
Gifu 501-1194, Japan
e-mail: ohnishih@gifu-u.ac.jp

H. Iwata · M. Seishima
Department of Dermatology, Graduate School of Medicine,
Gifu University,
Gifu, Japan

R. Nishikomori
Department of Pediatrics, Graduate School of Medicine,
Kyoto University,
Kyoto, Japan

H. Kaneko
Department of Clinical Research, Nagara Medical Center,
Gifu, Japan

Published online: 24 December 2011

characteristic clinical phenotypes and examination of gene mutations in *NLRP3*. A hotspot of gene mutations in *NLRP3* is located on exon 3. On the other hand, approximately 40% of cases with the clinically diagnosed severe form of CAPS, chronic infantile neurologic cutaneous and articular (CINCA)/neonatal-onset multisystem inflammatory disease (NOMID) syndrome, have no detectable germline gene mutations in *NLRP3* [5, 6]. Some of these patients have gene mutations in *NLRP3* outside of exon 3, *NLRP12*, or somatic mosaicism of *NLRP3* [5, 7–10]. In some of the remaining typical CAPS patients, the disease-causing mutations cannot be confirmed. Thus, the clinical phenotypes are very important for diagnosing CAPS patients.

Familial cold autoinflammatory syndrome (FCAS) shows the mildest clinical phenotypes in the spectrum of CAPS, such as cold-induced urticaria-like skin rash, while CINCA/NOMID syndrome shows additional severe phenotypes, such as severe arthritis, patella overgrowth, aseptic meningitis, mental retardation, and progressive sensory neural hearing loss [1]. The diagnosis of FCAS is relatively difficult owing to its mild phenotypes compared with the more severe phenotypes of CAPS (CINCA/NOMID syndrome or Muckle–Wells syndrome (MWS)). On the other hand, and similar to other autoinflammatory syndromes such as familial Mediterranean fever, it is important for CAPS treatment to prevent the onset of renal amyloidosis for consideration of the prognosis. Interleukin (IL)-1β inhibitory drugs, such as anakinra, rilonacept, and canakinumab, can prevent the clinical phenotypes of CAPS including renal amyloidosis [11]. However, the usage of IL-1 blockade for the severe form of CAPS may sometimes be an overtreatment for FCAS because the clinical symptoms are relatively mild and the frequency of onset of renal amyloidosis was reported to be low in FCAS patients [11]. Therefore, precise evaluation of the disease severity of CAPS may contribute to a reduction in the usage of IL-1 blockade. Consequently, a convenient objective standard is anticipated for discrimination between the mild and severe forms of CAPS.

In this study, to diagnose CAPS and characterize the differences between the mild and severe forms of CAPS, we evaluated the serum inflammatory cytokine levels, cytokine production levels by peripheral blood mononuclear cells (PBMCs), and cell-based nuclear factor (NF)-κB reporter gene activities of *NLRP3* variants in patients. Our results provide new insights into the characterization of the severity of CAPS.

Methods

Case Reports

The five clinical cases evaluated in this study are described below, and their characteristics are summarized in Table I.

Table I Genotypes and clinical profiles of the patients

	Analyzed age	Onset age	Gender	Diagnosis	Genotype (*NLRP3*)	CNS		Skin	Joint	Others		The inflammatory markers	
						Meningitis	Mental retardation	Urticaria like rash	Arthritis	Hearing loss	Renal amyloidosis	WBC (/μl)	CRP (mg/dl)
Case 1	3 months	3 months	Female	FCAS	Y563N	−	−	+	−	−	−	14,890	0.48
Case 2	34 years	Unknown	Male	FCAS	Y563N	−	−	+	+	−	−	13,120	3.05
Case 3	14 years	11 months	Male	CINCA/NOMID	E688K, G809S	+	+	+	+	−	−	22,500	12.30
Case 4	45 years	Unknown	Female	MWS	E688K	−	−	+	+	+	−	13,640	4.17
Case 5	3 years	3 years	Female	JIA	E378K	−	−	+	+	−	−	15,200	11.69

CNS central nervous system, *FCAS* familiar cold inflammatory syndrome, *CINCA* chronic infantile neurologic cutaneous and articular syndrome, *MWS* Muckle–Wells syndrome, *JIA* juvenile idiopathic arthritis, *WBC* the count of white blood cells, *CRP* the serum C-reactive protein level

All of the patients' family members and healthy control subjects provided informed consent to participate in the study, and the ethical principles of the Declaration of Helsinki were followed.

Case 1 The onset of disease (FCAS) in this patient occurred at 3 months of age. She exhibited a recurrent generalized urticaria-like skin rash upon exposure to cold temperatures (Fig. 1a). Progressive sensory neural hearing loss and renal amyloidosis were not seen. Her serum C-reactive protein (CRP) levels were continuously and slightly increased (0.24–2.1 mg/dl).

Case 2 Case 2 was the father of case 1. He was a 34-year-old male with a recurrent urticaria-like skin rash, fever, conjunctivitis, and arthralgia that developed following fatigue or exposure to cold temperatures. The precise time of his disease onset was unknown. Progressive sensory neural hearing loss and renal amyloidosis were not seen [12]. His CRP levels were continuously increased (1.52–3.98 mg/dl).

Case 3 The onset of disease (CINCA/NOMID) in this patient occurred at 11 months of age. Continuous aseptic meningitis, urticaria-like skin rash, arthritis at the end of the fingers, and Raynaud's symptoms were observed. Arteriosclerosis of the ophthalmic artery was found. However, severe patella overgrowth was not seen. At 14 years of age, he had heart failure with myocarditis, which was considered to be a rheumatic characteristic. The patient died suddenly at 19 years of age (the detailed clinical case will be described elsewhere by Teramoto et al.).

Case 4 Case 4 was the mother of case 3. The precise time of her disease (MWS) onset was unknown. Initially, she was diagnosed with rheumatic arthritis and received oral prednisolone therapy. She suffered progressive sensory neural hearing loss at 30 years of age and underwent artificial cochlea replacement therapy at 48 years of age. This was greatly effective in improving her hearing ability. Meningitis and renal amyloidosis were not seen.

Case 5 The onset of disease in this patient occurred at 3 years of age. Fever that continued for more than 2 weeks, severe polyarthritis (serum matrix metalloproteinase-3 of >800 ng/ml), and recurrent urticaria-like non-itchy skin rash (Fig. 1b) were observed. Lymphadenopathy, hepatosplenomegaly, and serositis were not seen. Patella overgrowth, aseptic meningitis, progressive sensory neural hearing loss, and renal amyloidosis were not seen. Rheumatoid factor was negative. Other autoantibodies, including anticyclic citrullinated peptide antibody, were not detected. Her serum CRP and ferritin levels were increased (11.69 mg/dl and 255.1 ng/ml, respectively). Based on the below-mentioned hereditary traits and the results of in vitro functional assays, we diagnosed this patient as juvenile idiopathic arthritis (JIA), according to the criteria for JIA from the International League of Associations for Rheumatology [13]. A combination therapy with steroid and tocilizumab was effective.

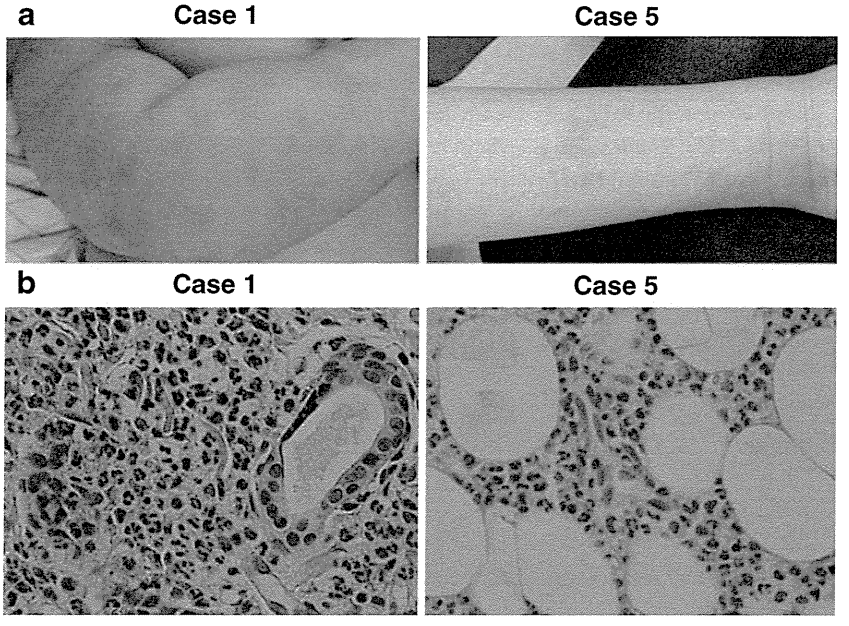

Fig. 1 Urticaria-like skin rash of cases 1 and 5. **a** Clinical appearances of the urticaria-like rash of cases 1 and 5. **b** Histopathological examinations of biopsy specimens from the skin rash of cases 1 and 5. Both skin biopsies show a recurrent cold-induced non-itchy urticaria-like skin rash and also show neutrophil infiltration

DNA Sequencing

Genomic DNA was extracted from leukocytes using Sepa-Gene (Eidia, Tokyo, Japan). A DNA fragment of the *NLRP3* gene was amplified by PCR and analyzed using Big Dye Terminator Bidirectional Sequencing (Applied Biosystems, Foster City, CA, USA).

Cell Culture

PBMCs were isolated from heparinized blood from control donors and patients by gradient centrifugation in Ficoll-Paque (GE Healthcare, Uppsala, Sweden). The PBMCs were cultured in medium consisting of RPMI 1640 supplemented with 10% heat-inactivated fetal calf serum, L-glutamine (2 mmol/l), penicillin (100 U/ml), and streptomycin (100 pg/ml). Human embryonic kidney (HEK) 293T cells were cultured in Dulbecco's modified Eagle's medium (high glucose-containing DMEM; Invitrogen, Carlsbad, CA, USA) supplemented with 10% heat-inactivated fetal bovine serum (Sigma-Aldrich, St. Louis, MO, USA), penicillin (100 U/ml), and streptomycin (100 μg/ml).

Vector Preparations

A cDNA encoding *NLRP3* tagged at the C terminus with a FLAG epitope (NLRP3-FLAG) was cloned into the plasmid vector pcDNA3.1+ (Invitrogen). Mutants of *NLRP3* (E378K, Y563N, E688K, and G809S) were generated using a GeneEditor In Vitro Site-Directed Mutagenesis System (Promega, Madison, WI, USA). An ASC variant 1 tagged at the C terminus with a myc epitope (ASC1-myc) was also cloned into pcDNA3.1+. An NF-κB luciferase reporter vector (pGL4.32-luc2P/NF-kappaB-RE/Hygro) and a *Renilla* luciferase reporter vector (pGL4.74-hRluc/TK) were purchased from Promega.

NF-κB Reporter Gene Activity

HEK293T cells in 96-well plates were transfected with 16 ng/well of pcDNA3.1+ control vector or pcDNA3.1+ NLRP3-FLAG vector (wild-type or mutant-type) using Lipofectamine 2000 (Invitrogen), according to the manufacturer's instructions. The pcDNA3.1+ ASC1-myc vector, NF-κB luciferase reporter vector, and *Renilla* luciferase reporter vector were cotransfected. After transfection, the cells were cultured for 24 h. The luciferase reporter gene activities were analyzed using a Dual-Luciferase Reporter Assay System (Promega). The statistical significance of differences in the luciferase activities between the wild-type and mutant genes in the NF-κB gene reporter assays was analyzed by the Kruskal–Wallis test, and further analysis was performed by the Bonferroni/Dunn test. Statistical significance was assumed for values of $P<0.05$.

Lipopolysaccharide- or Hypothermia-Induced Assays

PBMCs were suspended at 1×10^6 cells/ml in culture medium and cultured in the presence or absence of 10 or 100 ng/ml of LPSO127 (Sigma) for 24 h in six-well plates at 30°C or 37°C in a humidified atmosphere containing 5% CO_2.

Measurements of Tumor Necrosis Factor-α, IL-6, IL-1β, IL-1ra, and IL-18

Sera from the patients and healthy control subjects ($n=10$; age range, 1–35 years) were stored at −80°C until analysis. The sera of cases 1 and 2 were collected when they had the cold-induced rash, but not fever. The sera of cases 3, 4, and 5 were collected during a fever episode as an autoinflammatory symptom. Culture supernatants in test tubes or microtest plates were centrifuged to remove the cells and then stored at −80°C until analysis. The tumor necrosis factor (TNF)-α, IL-6, IL-1β, IL-1ra, and IL-18 concentrations were measured using a Human TNF-α Immunoassay Kit (BioSource, Camarillo, CA, USA), Human IL-6 Immunoassay Kit (BioSource), Human IL-1β Immunoassay Kit (BioSource), Quantikine Human IL-1ra/IL-1F3 ELISA Kit (R&D Systems, Minneapolis, MN, USA), and Human IL-18 ELISA Kit (MBL, Nagoya, Japan), respectively. The detection limits of the cytokine measurement kits were as follows: TNF-α, 1.7 pg/ml; IL-6, 2.0 pg/ml; IL-1β, 1.0 pg/ml; IL-1ra, 6.26 pg/ml; IL-18, 12.5 pg/ml. Values under the detection limits were shown as not detected. The serum cytokine levels were measured at two points at least, and the average values were calculated. The cytokine production levels by PBMCs were measured in duplicate and the average values were calculated. We defined cytokine levels of more than the mean+2 SD as increasing.

Results

Detection of Gene Variations in *NLRP3*

In the five patients, four heterozygous missense variations (E378K, Y563N, E688K, and G809S) of the *NLRP3* gene were identified (Table I). Interestingly, case 3 showed compound heterozygous gene variations, E688K and G809S, while his mother (case 4) had only one mutation, E688K, of *NLRP3*. The G809S allele was inherited from his asymptomatic father. In case 5, a novel missense variation, E378K, in *NLRP3* was identified. In addition, a heterozygous mutation, E148Q, in *MEFV* was identified. Gene mutations in *TNFRSF1A*, *MVK*, *NLRP12*, and *NOD2* were not found.

The genotypes of *NLRP3* and *MEFV* in her asymptomatic mother were the same. It should be noted that E378K and G809S were not present in the *INFEVERS* database (http://fmf.igh.cnrs.fr/ISSAID/infevers/) [14] and were confirmed as rare variants that were not identified in the 100 ethnically matched control subjects.

NF-κB Reporter Gene Activities of the *NLRP3* Variants

Figure 2 shows the ASC-dependent NF-κB activities of the *NLRP3* variants in vitro. The NF-κB reporter gene activities were increased by the Y563N and E688K mutations in *NLRP3*. The activities were higher for D303N (as a positive control *NLRP3* mutation that was previously identified in a CINCA/NOMID patient [5]) and E688K than for the FCAS mutation, Y563N. E378K and G809S did not cause any significant increases in the activities. Initially, we suspected that case 5 had CAPS. However, based on these results, we were able to confirm the diagnosis of case 5 as JIA, rather than CAPS.

Cytokine Profiles of the Patients

The serum IL-1β, IL-6, and TNF-α levels were not detected in the sera of the healthy control subjects. Although we were unable to detect IL-1β in the patients' sera, we clearly detected the serum IL-18 and IL-1ra levels in all cases (Fig. 3a, b). The serum IL-18 levels were extremely high in the CINCA/NOMID (case 3), MWS (case 4), and JIA (case 5) patients compared with the control subjects. The serum IL-1ra and IL-6 levels were increased in cases 2, 3, 4, and 5 (Fig. 3b, c). The serum TNF-α levels were increased in cases 1, 2, and 3 (Fig. 3d).

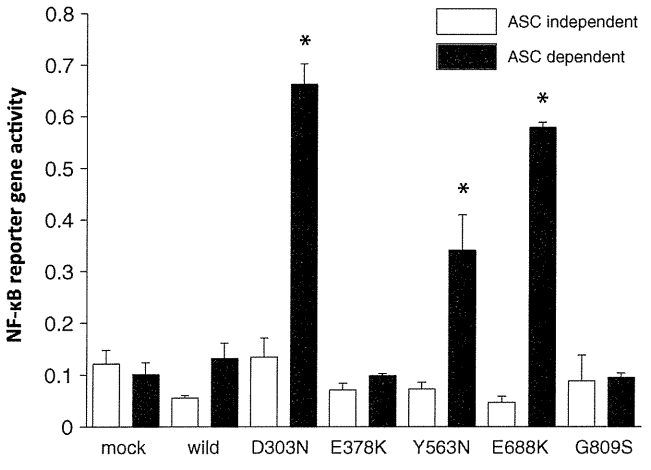

Fig. 2 NF-κB reporter gene activities of the *NLRP3* variants. The *white bars* indicate the NF-κB reporter gene activities of the *NLRP3* variants without cotransfection of ASC, while the *black bars* indicate these activities with cotransfection of ASC. The data shown are the means±SD of triplicate assays. The ASC-dependent NF-κB reporter gene activities are increased for the variants with D303N, Y563N, and E688K. The activities for the CINCA/NOMID mutations, D303N and E688K, are higher than those for the FCAS mutation, Y563N. The variants with E378K and G809S do not show any significant increases in the activities. *$P<0.05$

Interestingly, the serum IL-18 levels in the FCAS patients (cases 1 and 2) did not show any increases compared with the control subjects (Fig. 3a). Furthermore, the levels of spontaneous IL-1β production by PBMCs from the CINCA/NOMID (case 3) and MWS (case 4) patients were increased, whereas those of the control subjects, FCAS patients, and JIA patient (cases 1, 2, and 5) did not show any increases (Fig. 4a).

The lipopolysaccharide (LPS)-induced cytokine production levels by PBMCs from the FCAS and JIA patients are shown in Fig. 4b–d. The IL-1β and IL-18 production levels were increased in the FCAS patients compared with the control subjects. However, TNF-α did not show any significant changes. Comparisons of the cytokine production levels by the PBMCs cultured at 30°C and 37°C are shown in Fig. 5. The PBMCs from the FCAS patients showed obvious increases in the IL-1β and IL-18 production levels after culture at the lower temperature with no stimulation.

Discussion

The diagnosis of CAPS is still based on the clinical symptoms and recognition of a syndrome. Detection of a pathogenic *NLRP3* mutation can confirm the CAPS diagnosis. However, to confirm the diagnosis of CAPS patients with novel identified *NLRP3* variations, some functional experiments regarding the effects of the *NLRP3* mutations, such as the NF-κB luciferase reporter gene assay used in this study, are necessary because of the existence of nonfunctional missense variations of *NLRP3* [7]. Furthermore, although there are many previously reported missense mutations of *NLRP3* associated with CAPS in the *INFEVERS* database [14], the mutations with confirmed functional evidence are limited. In this study, we identified *NLRP3* gene mutations in five patients who were suspected of having autoinflammatory syndromes. Two mutations of *NLRP3*, Y563N and E688K, were previously reported to be disease-causing mutations [15, 16], although in vitro functional assays were not performed. Y563N was first identified in FCAS patients who were diagnosed based on the clinical criteria of FCAS [16, 17]. Our FCAS patients (cases 1 and 2) showed a skin rash, occasional fever, and mild arthritis and did not show any severe symptoms, such as neurological disorders, hearing loss, and renal amyloidosis. On the other hand, E688K was first identified in an Italian male CINCA/NOMID patient [15] who was described as having a skin rash, hearing loss, fever, and transient arthritis without persistent deformities of the involved joints. Our patients with E688K

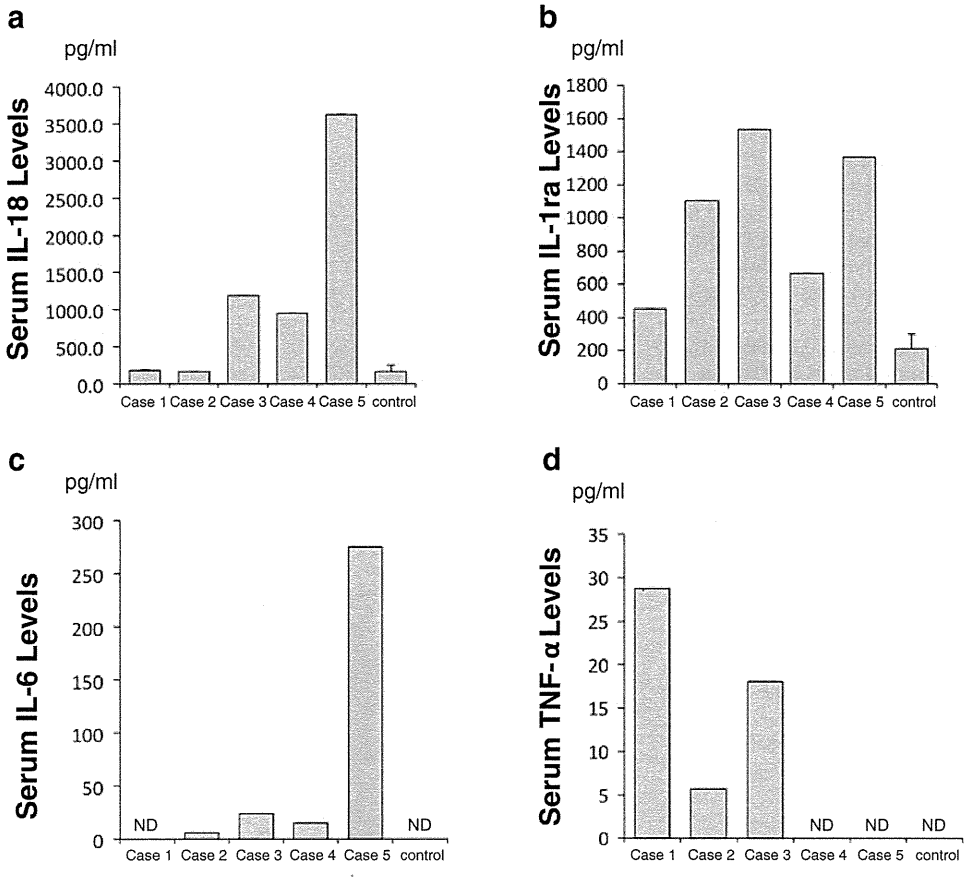

Fig. 3 Serum inflammatory cytokines in the four CAPS cases. IL-1β, IL-6, and TNF-α were not detected in the sera of the control subjects. The means ±D of the serum IL-18 and IL-1ra levels of the healthy control subjects were 169.2±85.7 and 213.4±87.1 pg/ml, respectively (n=10)

(cases 3 and 4) also had no strong deformities of the joints, but had obviously more severe phenotypes than FCAS, such as aseptic meningitis and hearing loss. In the present study, the E688K mutation in the MWS and CINCA/NOMID syndrome patients showed significantly stronger NF-κB activities than the Y563N mutation identified in the FCAS patients. Our findings indicate that the clinical phenotypes and values of the ASC-dependent NF-κB activity assay are well correlated with the genetic mutations, consistent with a previous report [18]. However, the artificial reporter gene assay system used may have little to do with the function of the CAPS pathophysiology, and limited numbers of *NLRP3* variants have been assessed using the assay in the present and previous studies, thereby making it difficult to prove this hypothesis at the present time. Consequently, further experiments including large amounts of pathogenic mutations and accumulation of detailed clinical information about the disease severity of CAPS are necessary to confirm this hypothesis. It should be noted that low-penetrance mutation, G809S, did not show positive activity with this in vitro assay system. But the clinical phenotype of case 3 was obviously more severe than case 4, although the father of case 3, who also was found to have G809S, was as symptomatic. Because of the discrepancy between the patient and the father, it remains unclear whether G809S is a pathogenic mutation or, alternatively, if there is an alternative genetic explanation for disease in the patient not detected by genomic DNA sequencing.

On the other hand, it requires time to build the above-mentioned in vitro experimental system. For the rapid diagnosis and characterization of CAPS, a simple screening system is necessary. In this study, we measured several serum inflammatory cytokine levels in our patients (Fig. 3). The serum IL-6 level is usually used for evaluating the disease severity of rheumatoid arthritis [19]. Moreover, the serum IL-18 level was recently reported to reflect the disease severity of not only JIA but also other diseases such as allergic diseases [20, 21]. In our CAPS patients, the serum levels of IL-18, but not IL-1β, seemed to be correlated with the disease phenotypes. Although the precise reason for this dissociation between the IL-18 and IL-1β levels in the sera is unknown, IL-1β may be rapidly neutralized, metabolized, or captured by a plethora of IL-1 receptors in vivo. In fact, serum IL-1ra, which is the counter-regulator of IL-1, was increased in our CAPS patients. Thus, the serum IL-18 levels may be used as an appropriate marker for the evaluation of treatments, although it is unlikely that serum IL-18 can contribute to the differential diagnosis between CAPS and other diseases.

The diagnosis of FCAS seems to be relatively difficult because of its mild phenotypes compared with the other more severe phenotypes of CAPS. The serum inflammatory

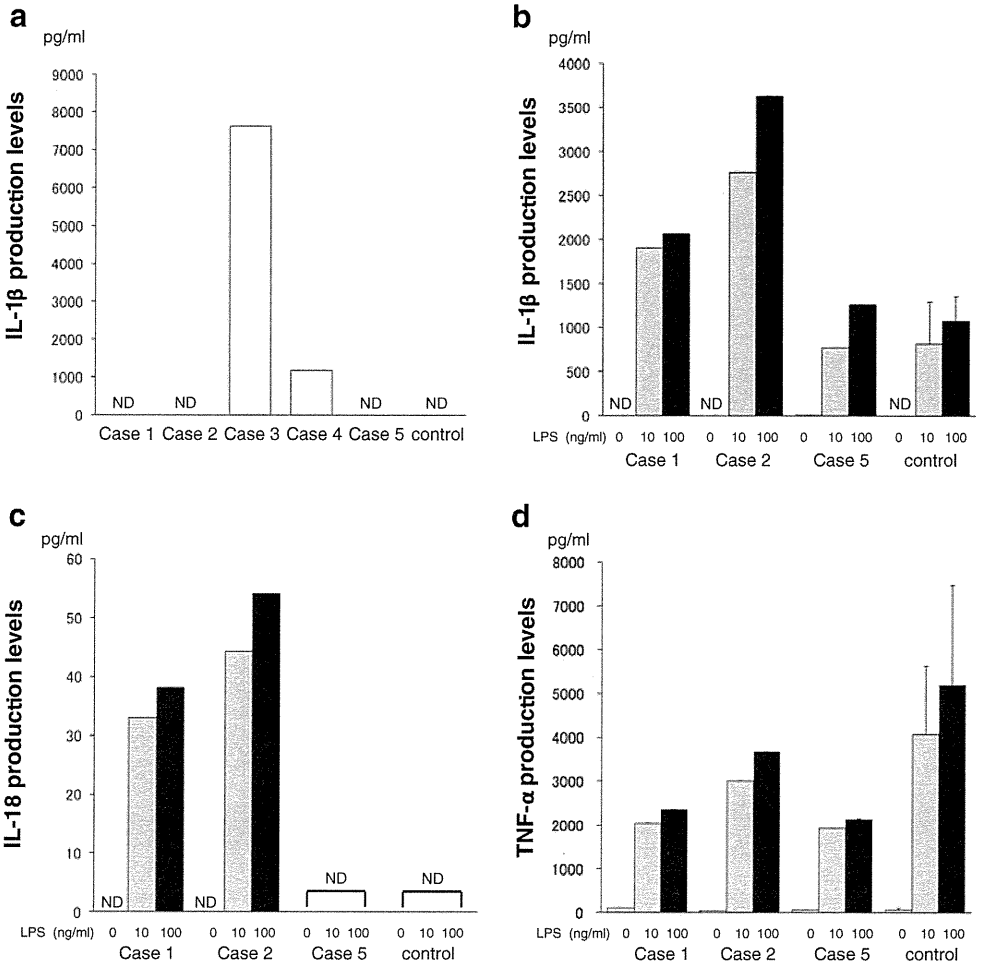

Fig. 4 LPS-induced cytokine production levels in the patients. **a** The *white bars* indicate the spontaneous IL-1β production levels by PBMCs. Increased IL-1β production by PBMCs from case 3 (CINCA/NOMID syndrome) and case 4 (MWS) is detected, whereas no increases are observed for the PBMCs from the control subjects and cases 1, 2 (FCAS), and 5 (JIA). **b**, **c** The LPS-induced IL-1β and IL-18 production levels by PBMCs from the FCAS patients are increased compared with PBMCs from the control subjects. **d** The TNF-α production levels by PBMCs from the FCAS and JIA patients do not show any significant changes. In **b–d**, the *white bars* indicate the cytokine production levels without stimulation and the *gray* and *black bars* indicate the cytokine production levels after stimulation by 10 and 100 ng/ml LPS, respectively

cytokine levels in our FCAS patients did not show any typical increases, unlike the case for the CINCA/NOMID patient (Fig. 3), indicating that the establishment of an effective and easy screening method is important for the diagnosis of FCAS. Therefore, we focused on the cytokine production levels in these patients' blood cells. First, IL-1β production by nonstimulated PBMCs was observed in our CINCA/NOMID and MWS patients (cases 3 and 4, respectively), as reported previously [5]. However, no enhancement of spontaneous IL-1β production was observed in our FCAS patients (cases 1 and 2) (Fig. 4a), suggesting that this method may not be suitable for screening of FCAS.

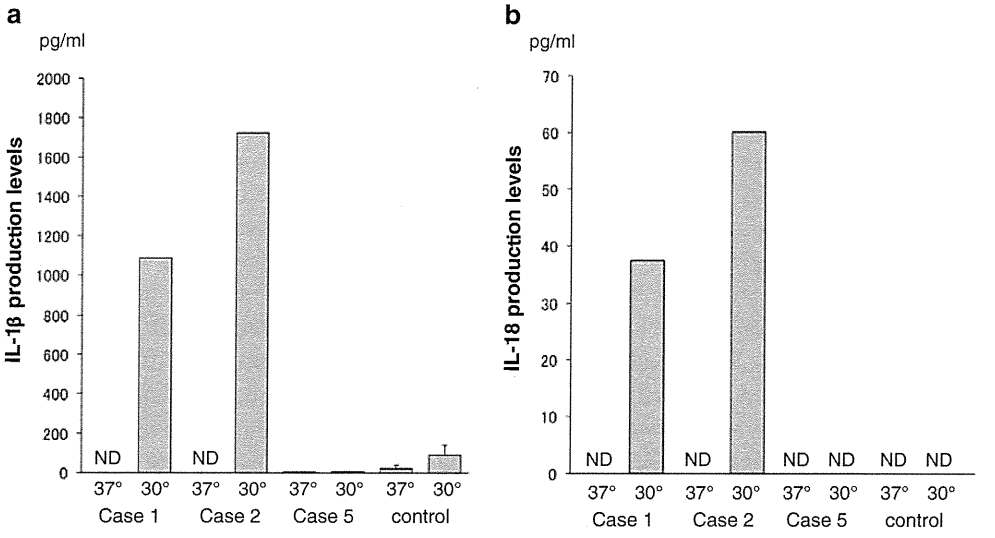

Fig. 5 Hypothermia-induced cytokine production levels by PBMCs from the FCAS and JIA patients. **a**, **b** Comparisons of the cytokine production levels by PBMCs cultured at 30°C and 37°C. The PBMCs from the FCAS patients (cases 1 and 2) show obvious increases in the IL-1β and IL-18 production levels after culture at lower temperature with no stimulation

Furthermore, the LPS- or hypothermia-induced cytokine production levels by the PBMCs showed marked elevation of IL-1β or IL-18 (Figs. 4a–c and 5b), as reported previously [16, 22]. The phenomena for hypothermic culture were similar to the findings in our recent report that NF-κB activity induced by LPS stimulation through TLR4 is enhanced in low-temperature cultures [23], although the precise mechanism of the association between the *NLRP3* variations and the low-temperature stimulation requires further clarification. These findings suggest that the cytokine production assays induced by LPS or hypothermia stimulation should be helpful for the diagnosis of FCAS. It should be noted that the serum IL-18 levels could be detected in all of the non-CAPS subjects, although the production levels of IL-18 from their PBMCs were lower than the detection limit. This might be dependent on the long half-life of IL-18 in human blood compared with the above-mentioned half-life of IL-1β.

The discrimination between CAPS and JIA cases is sometimes difficult because of their similar clinical characteristics. Interestingly, although case 5 had a rare missense variation in *NLRP3* (E378K) and some of her clinical symptoms were similar to those of CAPS (Table I), the E378K variant did not show enhancement of NK-κB activity (Fig. 2). This gene variation was inherited from her mother who did not show any inflammatory symptoms. Case 5 showed strong polyarthritis, continuous fever, and a recurrent generalized urticaria-like erythema as well as symptoms of CAPS. In particular, histopathological examination of a biopsy specimen from her skin rash revealed infiltration of neutrophils and mononuclear cells, representing similar findings to case 1 (Fig. 1). Thus, it was difficult to discriminate CAPS by the clinical symptoms alone in this case.

Therefore, to discriminate between CAPS and JIA in this case, we focused on her cytokine profiles. Her serum IL-6 and IL-18 levels were extremely high compared with not only the healthy controls but also the other CAPS patients (Fig. 3a, c). These observations resembled the serum cytokine pattern of systemic-onset JIA [21, 24]. Furthermore, the LPS-induced and hypothermia-induced IL-1β and IL-18 production levels by PBMCs from case 5 showed no increases compared with the control subjects (Figs. 4b, c and 5a, b). Recently, Saito et al. [5] reported that another screening method, LPS-induced monocyte cell death, was effective for diagnosing CAPS. The monocytes in case 5 did not show LPS-induced cell death. These objective results also supported the diagnosis of case 5 as JIA, rather than CAPS.

In this study, we evaluated several methods for the limited genotypes of patients with *NLRP3* variants. According to comparisons of the clinical phenotypes of previous case reports and our cases, the disease severity seems to be correlated with the serum cytokine levels and the ex vivo and in vitro responses and is almost completely determined by the specific mutations, which appear to suggest that other genetic or epigenetic determinants or environmental factors do not play a significant role.

Conclusions

A precise and easy method for the diagnosis of CAPS has not yet been established. The characteristics of the clinical phenotypes and the identification of proven gene variations of *NLRP3*, as the etiology of CAPS, are very important for diagnosing CAPS. In addition, the serum IL-18 levels and NF-κB activities of patients with the *NLRP3* variants reflect the phenotypes of disease severity. Evaluation of the cytokine profile is also a useful tool for diagnosing and discriminating the severity of CAPS.

Acknowledgements We thank the members of the families who agreed to participate in the study. We thank Dr. T. Fukao, Dr. M. Kawamoto, Dr. N. Kawamoto, and K. Kasahara for their advice and technical help. This work was supported by Grants-in-Aid for Scientific Research from the Ministry of Education, Science and Culture of Japan and by Health and Labour Science Research Grants for Research on Intractable Diseases from the Ministry of Health, Labour and Welfare.

Conflicts of Interest The authors have declared no conflicts of interest.

References

1. Hoffman HM, Simon A. Recurrent febrile syndromes: what a rheumatologist needs to know. Nat Rev Rheumatol. 2009;5:249–56.
2. Aksentijevich I, Nowak M, Mallah M, Chae JJ, Watford WT, Hofmann SR, et al. De novo CIAS1 mutations, cytokine activation, and evidence for genetic heterogeneity in patients with neonatal-onset multisystem inflammatory disease (NOMID): a new member of the expanding family of pyrin-associated autoinflammatory diseases. Arthritis Rheum. 2002;46:3340–8.
3. Feldmann J, Prieur AM, Quartier P, Berquin P, Certain S, Cortis E, et al. Chronic infantile neurological cutaneous and articular syndrome is caused by mutations in CIAS1, a gene highly expressed in polymorphonuclear cells and chondrocytes. Am J Hum Genet. 2002;71:198–203.
4. Hoffman HM, Mueller JL, Broide DH, Wanderer AA, Kolodner RD. Mutation of a new gene encoding a putative pyrin-like protein causes familial cold autoinflammatory syndrome and Muckle–Wells syndrome. Nat Genet. 2001;29:301–5.
5. Saito M, Nishikomori R, Kambe N, Fujisawa A, Tanizaki H, Takeichi K, et al. Disease-associated CIAS1 mutations induce monocyte death, revealing low-level mosaicism in mutation-negative cryopyrin-associated periodic syndrome patients. Blood. 2008;111:2132–41.
6. Tanaka N, Izawa K, Saito MK, Sakuma M, Oshima K, Ohara O, et al. High incidence of NLRP3 somatic mosaicism in chronic infantile neurological cutaneous and articular syndrome patients: the

results of an international multicenter collaborative study. Arthritis Rheum. 2011;63:3625–32.
7. Saito M, Fujisawa A, Nishikomori R, Kambe N, Nakata-Hizume M, Yoshimoto M, et al. Somatic mosaicism of CIAS1 in a patient with chronic infantile neurologic, cutaneous, articular syndrome. Arthritis Rheum. 2005;52:3579–85.
8. Matsubayashi T, Sugiura H, Arai T, Oh-Ishi T, Inamo Y. Anakinra therapy for CINCA syndrome with a novel mutation in exon 4 of the CIAS1 gene. Acta Paediatr. 2006;95:246–9.
9. Jeru I, Duquesnoy P, Fernandes-Alnemri T, Cochet E, Yu JW, Lackmy-Port-Lis M, et al. Mutations in NALP12 cause hereditary periodic fever syndromes. Proc Natl Acad Sci USA. 2008;105:1614–9.
10. Jeru I, Marlin S, Le Borgne G, Cochet E, Normand S, Duquesnoy P, et al. Functional consequences of a germline mutation in the leucine-rich repeat domain of NLRP3 identified in an atypical autoinflammatory disorder. Arthritis Rheum. 2010;62:1176–85.
11. Church LD, Savic S, McDermott MF. Long term management of patients with cryopyrin-associated periodic syndromes (CAPS): focus on rilonacept (IL-1 Trap). Biologics. 2008;2:733–42.
12. Yamauchi A, Iwata H, Ohnishi H, Teramoto T, Kondo N, Seishima M. Interleukin-17 expression in the urticarial rash of familial cold autoinflammatory syndrome: a case report. Br J Dermatol. 2010;163:1351–3.
13. Petty RE, Southwood TR, Baum J, Bhettay E, Glass DN, Manners P, et al. Revision of the proposed classification criteria for juvenile idiopathic arthritis: Durban, 1997. J Rheumatol. 1998;25:1991–4.
14. Milhavet F, Cuisset L, Hoffman HM, Slim R, El-Shanti H, Aksentijevich I, et al. The infevers autoinflammatory mutation online registry: update with new genes and functions. Hum Mutat. 2008;29:803–8.
15. Caroli F, Pontillo A, D'Osualdo A, Travan L, Ceccherini I, Crovella S, et al. Clinical and genetic characterization of Italian patients affected by CINCA syndrome. Rheumatol Oxford. 2007;46:473–8.
16. Rosengren S, Mueller JL, Anderson JP, Niehaus BL, Misaghi A, Anderson S, et al. Monocytes from familial cold autoinflammatory syndrome patients are activated by mild hypothermia. J Allergy Clin Immunol. 2007;119:991–6.
17. Hoffman HM, Wanderer AA, Broide DH. Familial cold autoinflammatory syndrome: phenotype and genotype of an autosomal dominant periodic fever. J allergy clin immunol. 2001;108:615–20.
18. Kambe N, Satoh T, Tanizaki H, Fujisawa A, Saito MK, Nishikomori R. Enhanced NF-kappaB activation with an inflammasome activator correlates with disease activity of NLRP3 mutations outside of exon 3: comment on an article by Jeru et al. Arthritis Rheum. 2010;62:3123–4.
19. Madhok R, Crilly A, Watson J, Capell HA. Serum interleukin 6 levels in rheumatoid arthritis: correlations with clinical and laboratory indices of disease activity. Ann Rheum Dis. 1993;52:232–4.
20. Tanaka H, Miyazaki N, Oashi K, Teramoto S, Shiratori M, Hashimoto M, et al. IL-18 might reflect disease activity in mild and moderate asthma exacerbation. J Allergy Clin Immunol. 2001;107:331–6.
21. Lotito AP, Campa A, Silva CA, Kiss MH, Mello SB. Interleukin 18 as a marker of disease activity and severity in patients with juvenile idiopathic arthritis. J Rheumatol. 2007;34:823–30.
22. Janssen R, Verhard E, Lankester A, Ten Cate R, van Dissel JT. Enhanced interleukin-1beta and interleukin-18 release in a patient with chronic infantile neurologic, cutaneous, articular syndrome. Arthritis Rheum. 2004;50:3329–33.
23. Arai T, Kaneko H, Ohnishi H, Matsui E, Fukao T, Kawamoto N, et al. Hypothermia augments NF-kappaB activity and the production of IL-12 and IFN-gamma. Allergol Int. 2008;57:331–8.
24. Yilmaz M, Kendirli SG, Altintas D, Bingol G, Antmen B. Cytokine levels in serum of patients with juvenile rheumatoid arthritis. Clin Rheumatol. 2001;20:30–5.

JOURNAL OF CLINICAL MICROBIOLOGY, Sept. 2011, p. 3432–3435 Vol. 49, No. 9
0095-1137/11/$12.00 doi:10.1128/JCM.00478-11

Refractory Chronic Pleurisy Caused by *Helicobacter equorum*-Like Bacterium in a Patient with X-Linked Agammaglobulinemia▽

Michinori Funato,[1]* Hideo Kaneko,[1] Kiyofumi Ohkusu,[2] Hideo Sasai,[1] Kazuo Kubota,[1] Hidenori Ohnishi,[1] Zenichiro Kato,[1,3,4] Toshiyuki Fukao,[1,5] and Naomi Kondo[1,3,4]

Department of Pediatrics[1] and Department of Microbiology,[2] Graduate School of Medicine, Gifu University, Gifu, Japan; Center for Emerging Infectious Diseases[3] and Center for Advanced Drug Research,[4] Gifu University, Gifu, Japan; Medical Information Sciences Division, United Graduate School of Drug Discovery and Medical Information Sciences, Gifu University, Gifu, Japan[5]; and Department of Clinical Research, National Hospital Organization, Nagara medical Center, Gifu, Japan[6]

Received 9 March 2011/Returned for modification 6 April 2011/Accepted 6 June 2011

We describe a 35-year-old man with X-linked agammaglobulinemia who had refractory chronic pleurisy caused by a *Helicobacter equorum*-like bacterium. Broad-range bacterial PCR targeting the 16S and 23S rRNA genes and *in situ* hybridization targeting the 16S rRNA gene of *H. equorum* confirmed the presence of this pathogen in a human for the first time.

CASE REPORT

A 35-year-old man was referred to us for a low-grade fever, fatigue, and discomfort in the right thorax. He had been diagnosed with X-linked agammaglobulinemia (XLA) during the first year of life (5). Upon diagnosis, he showed extremely low serum immunoglobulin G, A, and M levels (650 mg/liter, under 80 mg/liter, and under 60 mg/liter, respectively) and had a missense mutation, L111R (464T>G), in Bruton's tyrosine kinase (BTK) gene (Fig. 1A). His family pedigree with respect to XLA is shown in Fig. 1B. Substitution therapy with intravenous immunoglobulin was administered every 4 weeks from his childhood. During his high school years, he had acute right pleurisy and a pleural puncture, but the details are unclear. In 2006, he suffered from right pleurisy again and then was repeatedly admitted to our hospital for 2 years. No pathogens causing his chronic pleurisy have ever been detected, even though some conventional cultures of blood and sputum have been performed. However, administration of panipenem/betamipron (PAPM/BP) had been the only way to improve his chest discomfort and transiently reduce C-reactive protein (CRP) levels. Administration of other antimicrobial treatments, such as the use of macrolides, cephems, newquinolones, glycopeptides, and carbapenems other than PAPM/BP, has resulted in no improvement.

On admission in 2008, his laboratory findings showed a normal white blood cell count (7.76×10^9/liter), a high CRP level (50.3 mg/liter), and a very high endotoxin level (131 ng/liter). A chest radiograph showed a thickened right pleura and pneumonia in the right inferior lung (Fig. 2A), and a computed tomography (CT) scan of the chest also showed the thickened right pleura with calcification and an alveolar opacity in the right inferior lung (Fig. 2B). We suspected a Gram-negative bacterial infection due to the transient PAPM/BP effectiveness and the high endotoxin level or *Mycobacterium tuberculosis* complex (MTC) infection due to the CT calcification finding. However, conventional cultures of blood, urine, sputum, and feces were all negative, as they had often been in the past.

A transbronchial lung biopsy and a transcutaneous pleural biopsy were performed for definite diagnosis. Histological examination of the alveolar spaces in the right lung showed intraluminal fibrosis of distal airspaces with foamy alveolar macrophages, suggesting secondary organizing pneumonia (OP) (Fig. 2C). In addition, examination of the right pleura showed chronic inflammation (Fig. 2D). Despite these findings, conventional bacterial cultures of biopsy samples from the right pleura grown in sheep blood agar (Nissui Pharmaceutical, Tokyo, Japan) and chocolate agar (Eiken Kagaku, Tokyo, Japan) plates showed no evidence of infection, and MTC cultures grown in an egg-based solid medium (Ogawa medium) (Kyokuto Pharmaceutical, Tokyo, Japan) was also negative.

To determine the pathogen of this refractory pleurisy, we performed broad-range bacterial PCR and mycobacterial PCR using the pleural samples. The PCR products targeting the bacterial 16S and 23S rRNA genes revealed a 1,473-bp band and a 563-bp band, respectively (Fig. 3A). Sequencing analysis was carried out using a GenBank BLAST search (National Center for Biotechnology, Bethesda, MD). Sequence editing and phylogenetic analyses were performed with ClustalW. The sequence of a 1,473-bp fragment of 16S rRNA gene confirmed the presence of *Helicobacter equorum*-like (99.8% identical) bacterium DNA (GenBank accession no. AB571486). Moreover, the sequence of a 563-bp fragment targeting the bacterial 23S rRNA gene was 98.9% similar to that of *H. equorum* (GenBank accession no. AB571487). On the other hand, PCR amplification of the 16S rRNA gene for MTC determinations was negative.

Next, to further demonstrate that the pleural infection involved an *H. equorum*-like bacterium, we performed *in situ* hybridization

* Corresponding author. Mailing address: Department of Pediatrics, Graduate School of Medicine, Gifu University, 1-1Yanagido, Gifu 501-1194, Japan. Phone: 81-58-2306386. Fax: 81-58-2306387. E-mail: mfunato@mac.com.

▽ Published ahead of print on 15 June 2011.

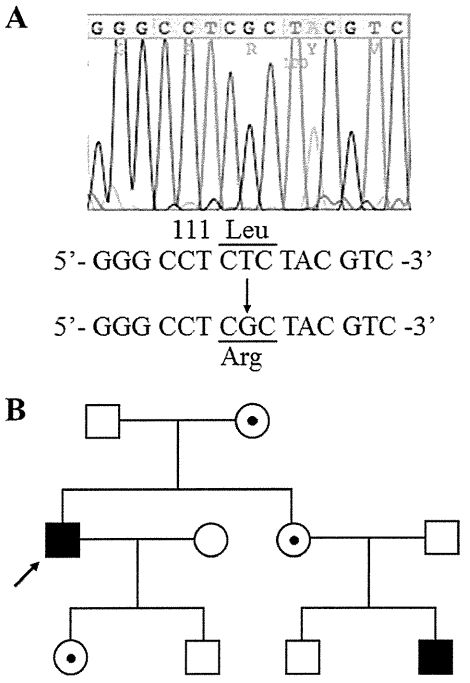

FIG. 1. Molecular analysis of the BTK gene and pedigree of our patient. (A) A missense mutation, L111R in BTK gene, identified in our patient. (B) The family tree for our patient. An arrow indicates the proband with XLA. The solid squares denote patients with XLA; circles with black dots denote mutation carriers.

using a digoxigenin-labeled single-strand RNA probe. The probe for positions 999 to 1118 in the 16S rRNA gene of *H. equorum* (GenBank accession no. AM998804) was designed as follows: 5′-UCCUCACCUUCCUCCUCCUUACGAAGGCAGUCUC CUUAGAGUGCUCAGCCAAACUGCUAGCAACUAAGG ACGAGGGUUGCGCUCGUUGCGGGACUUAACCCAAC AUCUCACGACACGAGC-3′. Positive signals in the pleural sample were confirmed with a nitroblue tetrazolium/5-bromo-4-chloro-3-indolylphosphate (NBT/BCIP) system (Roche Diagnostics, Tokyo, Japan) (Fig. 3B) but not in the control, which included the sense probe (Fig. 3C). These results indicated that the refractory chronic pleurisy in our patient was caused by an *H. equorum*-like bacterium, which in turn caused the development of secondary OP.

We began administration of PAPM/BP at a high dose of 8 g/day and of clarithromycin orally for 2 months. Since then, the patient has had no symptoms, and tests have shown negative CRP results and an endotoxin level of less than 10 ng/liter.

Since the discovery of *Helicobacter pylori* in 1984 (7), various *Helicobacter* species have been described in a wide variety of animal hosts, and transmission to humans has been suggested (3, 10, 14). In general, *Helicobacter pylori* is associated with gastritis, peptic ulcer disease, gastric adenocarcinoma, and mucosa-associated lymphoid tissue lymphoma (3). Also, non-*H. pylori Helicobacter* species are associated with gastric, intesti-

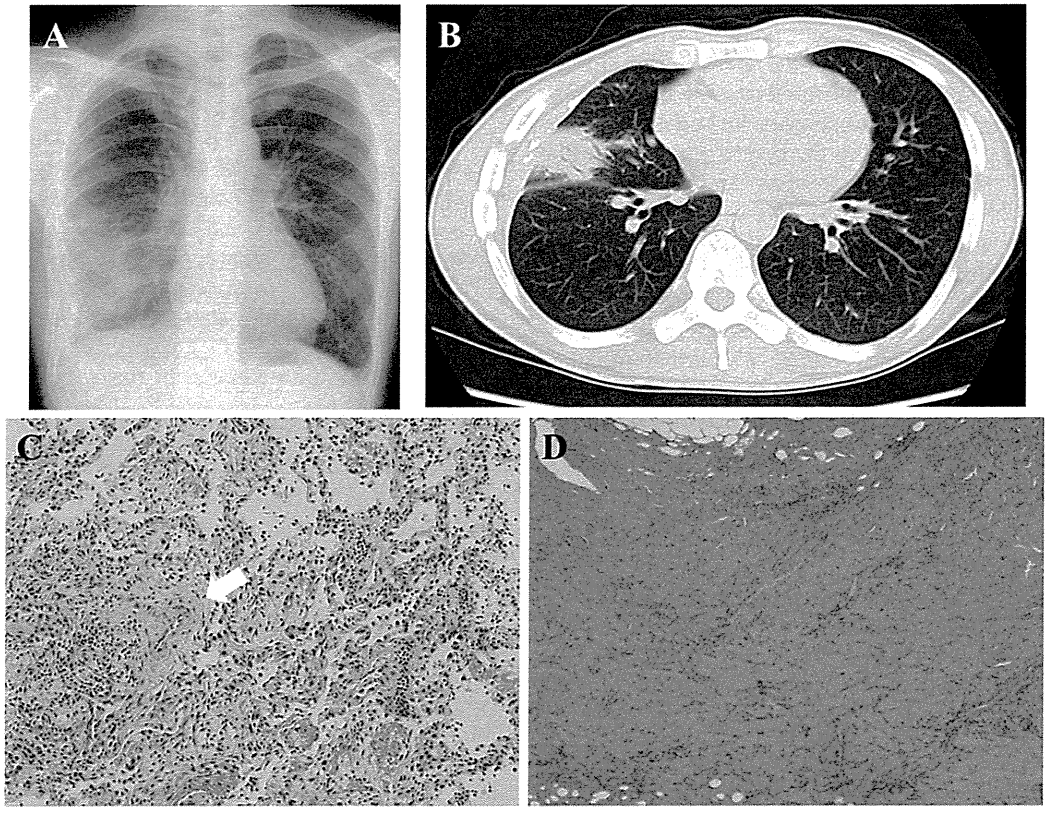

FIG. 2. Imaging and histological findings of refractory chronic pleurisy and secondary OP. (A and B) Results of a chest radiograph (A) and a chest CT scan (B) upon the latest admission of the patient to the hospital. (C) Histological finding in alveolar spaces, showing intraluminal fibrosis (arrow) (hematoxylin and eosin). (D) Histological finding in the right pleura, showing chronic inflammation (hematoxylin and eosin).

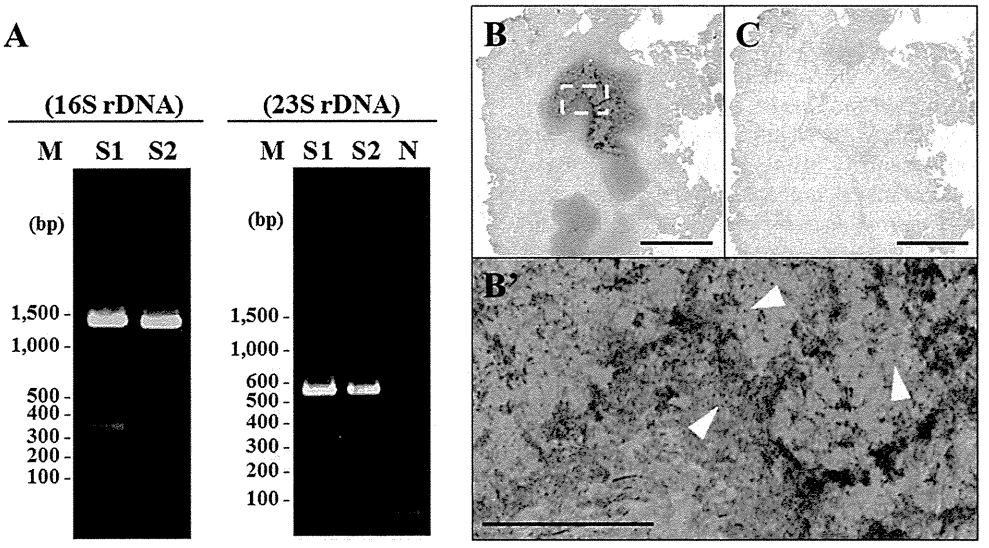

FIG. 3. Detection of *H. equorum*-like bacterium DNA in samples from the right pleura. (A) Broad-range bacterial products from a PCR targeting the 16S rRNA gene (left) and the 23S rRNA gene (right) determined using biopsy samples from the right pleura. S1 and S2 denote DNA samples from our patient. One-tenth the amount used in S1 was used in S2. N, negative control; M, marker. (B) Result of *in situ* hybridization of the pleural samples performed using the probe for the 16S rRNA gene of *H. equorum*. Scale bar, 500 μm. (B') Higher magnification of the bracketed areas shown in panel B. The signals of *H. equorum* were detected (arrowheads). Scale bar, 100 μm. (C) Negative control. Scale bar, 500 μm.

nal, and hepatobiliary diseases in humans (3, 10, 14). This understanding is attributed to molecular diagnosis based on the sequencing of bacterial 16S and 23S rRNA genes, an analytical technique that has already proved useful for various bacterial infections during antimicrobial treatment (11), for rare or unexpected pathogens (11), and particularly for difficult-to-culture bacteria such as non-*H. pylori Helicobacter* species (3). Herein, we have also described a case of refractory chronic pleurisy caused by an *H. equorum*-like bacterium that was subjected to molecular analysis.

Our patient had XLA, which is a rare genetic disorder of B-cell maturation characterized by the absence of mature B cells, very low serum levels of all immunoglobulin isotypes, and a lack of specific antibody production (6). He suffered for 2 years from right chronic pleurisy due to an unknown pathogen. We treated him with PAPM/BP on the basis of the clinical findings, but we were confused because the efficacy was transitory. Molecular diagnosis targeting bacterial 16S and 23S rRNA genes revealed that only DNA of an *H. equorum*-like bacterium that has not previously been reported to have been found in samples from humans was isolated from biopsy samples of our patient. Unfortunately, a culture for the *Helicobacter* species could not be performed for our patient because of the unexpected bacterium, but such culture is also difficult to perform in general, particularly for non-*H. pylori Helicobacter* species (3). We therefore performed *in situ* hybridization using the probe for the 16S rRNA gene of *H. equorum* and thereby confirmed that the infection had been caused by an *H. equorum*-like bacterium.

H. equorum, which is a Gram-negative, curved, and motile bacterium, was recently isolated from horse feces by molecular diagnosis (8). Additional investigation revealed that the prevalence of *H. equorum* was significantly higher in horses under veterinary care than in healthy horses, and *H. equorum* DNA has never been detected in human samples (9). To the best of our knowledge, this is the first case of infection with *H. equorum*-like bacterium in a human with XLA and in the respiratory system. So far, *Helicobacter* infections in patients with XLA have rarely been reported (2, 4, 12, 13), and none of those reported have been due to the presence of *Helicobacter* species in the respiratory system. Freeman and Holland illustrated the importance of humoral immunity in *Helicobacter* infections involving mucosal surfaces, because patients with XLA have been prone to chronic bacteremia, skin infections, and bone infections by the *Helicobacter* species (1). Our patient with XLA showed no evidence of bacteremia or other infections due to the presence of an *H. equorum*-like bacterium. In addition, the studied patient had not had any contact with horse feces, which is a possible vector of *H. equorum*, for the previous 2 years, though he had a history of right pleurisy. Finally, the source of the infection in our patient could not be identified, but we think it would be accurate to say that this infection, which exhibited abnormal humoral immunity, may have been associated with XLA.

Our patient with XLA has been treated with PAPM/BP, but we are unsure as to which antimicrobial treatment to use in a case like this. Because of the difficulty of performing culture, *in vitro* susceptibility testing has scarcely been evaluated or standardized for *H. equorum*. Moyaert et al. reported resistance to cephalotin and nalidixic acid and sensitivity to metronidazole for *H. equorum* (8). We also noted evidence of multiple drug resistance of this organism clinically, as our patient improved only after treatment with PAPM/BP; administration of many other antimicrobial treatments resulted in no improvement. Further investigation is needed, because antimicrobial treatment for *H. equorum* may be difficult.

In conclusion, we have described a case of chronic pleurisy associated with the presence of an *H. equorum*-like bacterium.

All of the clinical findings for our patient—transient PAPM/BP effectiveness, a high serum endotoxin level, and imaging-histological findings of chronic inflammation—were consistent with infections by this organism. This case illustrates both the usefulness of molecular diagnosis of infections with unknown organisms and the pathogenicity of the *H. equorum*-like bacterium in immunocompromised humans. In the future, the issues of whether *H. equorum* is associated with diseases in immunocompetent humans or not and of how patients infected with *H. equorum* are to be treated need to be investigated.

ACKNOWLEDGMENTS

We thank Yoshinobu Hirose, Yasushi Ohno, Kouyou Shirahashi, and Hisahi Iwata for contributing to the diagnosis and Hideki Hiraiwa for technical support with the *in situ* hybridization.

This work was supported by a grant from the Ministry of Health, Labor, and Welfare of Japan.

REFERENCES

1. **Freeman, A. F., and S. M. Holland.** 2007. Persistent bacterial infections and primary immune disorders. Curr. Opin. Microbiol. **10:**70–75.
2. **Gerrard, J., D. Alfredson, and I. Smith.** 2001. Recurrent bacteremia and multifocal lower limb cellulitis due to Helicobacter-like organisms in a patient with X-linked hypogammaglobulinemia. Clin. Infect. Dis. **33:**E116–E118.
3. **Haesebrouck, F., et al.** 2009. Gastric helicobacters in domestic animals and nonhuman primates and their significance for human health. Clin. Microbiol. Rev. **22:**202–223.
4. **Han, S., et al.** 2000. Identification of a unique Helicobacter species by 16S rRNA gene analysis in an abdominal abscess from a patient with X-linked hypogammaglobulinemia. J. Clin. Microbiol. **38:**2740–2742.
5. **Kanegane, H., et al.** 2001. Clinical and mutational characteristics of X-linked agammaglobulinemia and its carrier identified by flow cytometric assessment combined with genetic analysis. J. Allergy Clin. Immunol. **108:**1012–1020.
6. **Kaneko, H., et al.** 2005. Leaky phenotype of X-linked agammaglobulinaemia in a Japanese family. Clin. Exp. Immunol. **140:**520–523.
7. **Marshall, B. J., and J. R. Warren.** 1984. Unidentified curved bacilli in the stomach of patients with gastritis and peptic ulceration. Lancet **i:**1311–1315.
8. **Moyaert, H., et al.** 2007. Helicobacter equorum sp. nov., a urease-negative Helicobacter species isolated from horse faeces. Int. J. Syst. Evol. Microbiol. **57:**213–218.
9. **Moyaert, H., et al.** 2007. Prevalence of Helicobacter equorum in faecal samples from horses and humans. Vet. Microbiol. **121:**378–383.
10. **Okoli, A. S., A. Menard, and G. L. Mendz.** 2009. Helicobacter spp. other than Helicobacter pylori. Helicobacter **14:**69–74.
11. **Rantakokko-Jalava, K., et al.** 2000. Direct amplification of rRNA genes in diagnosis of bacterial infections. J. Clin. Microbiol. **38:**32–39.
12. **Schwarze-Zander, C., et al.** 2010. Bacteremia caused by a novel helicobacter species in a 28-year-old man with X-linked agammaglobulinemia. J. Clin. Microbiol. **48:**4672–4676.
13. **Simons, E., L. A. Spacek, H. M. Lederman, and J. A. Winkelstein.** 2004. Helicobacter cinaedi bacteremia presenting as macules in an afebrile patient with X-linked agammaglobulinemia. Infection **32:**367–368.
14. **Solnick, J. V.** 2003. Clinical significance of Helicobacter species other than Helicobacter pylori. Clin. Infect. Dis. **36:**349–354.

ADA-SCID with 'WAZA-ARI' mutations that synergistically abolished ADA protein stability

Adenosine deaminase (ADA) deficiency is a systemic purine metabolic disorder in which toxic levels of ADA substrates, particularly deoxyadenosine (dAdo), primarily affects lymphocyte development and functions (Hershfield & Mitchell, 2001). The affected patients present with varying degrees of immunodeficiency, such as severe combined immunodeficiency (ADA-SCID), delayed-onset ADA deficiency, and late-onset ADA deficiency. 'Partial ADA deficiency' has also been identified in healthy individuals with abolished ADA activity in erythrocytes but at greater levels in other cells (0·9–70% of normal) (Daddona *et al*, 1983; Hirschhorn & Ellenbogen, 1986). To date, more than 70 *ADA* mutations have been identified, including deletions, missense, nonsense, and splicing mutations (Hershfield, 2003). Correlation between the effect of mutations on ADA activity and clinical phenotype has been demonstrated by systematic expression studies of mutant *ADA* cDNAs in *Escherichia coli* (Arredondo-Vega *et al*, 1998; Hershfield, 2003). Here, we report an ADA-SCID patient with two mutations on the same allele, each of which retained detectable levels of ADA activity.

A Japanese 1-month-old boy was referred to our hospital because of poor sucking and failure to thrive. His elder brother had died of recurrent pneumonia at 4 months of age. His non-consanguineous parents and his younger sister were all in good health. Based on the history of his affected sibling, initial investigations were performed soon after birth. Although the initial haematological examination showed no lymphopenia (absolute lymphocyte count: $2{\cdot}79 \times 10^9$/l), profound lymphopenia (absolute lymphocyte count: $0{\cdot}13 \times 10^9$/l) was noticed when he was 40 d old. T-cell receptor excision circles were undetectable (Morinishi *et al*, 2009). After obtaining informed consent for genetic analysis under a protocol approved by the Institutional Review Board of Hokkaido University Graduate School of Medicine, we performed genetic analysis of T-B-SCID (SCID with a virtual lack of circulating mature T and B lymphocytes)-related genes, such as *ADA*, *RAG1*, *RAG2*, and *DCLRE1C*, and found mutations in *ADA* gene. He was diagnosed with ADA-SCID based on his clinical severity, immune dysfunction, and the presence of *ADA* mutations. He died of respiratory distress 22 d after unrelated umbilical cord blood stem cell transplantation.

Direct sequence analysis of the patient's genomic DNA demonstrated three base changes in the *ADA* gene: 355C>T (Q119X) in exon 4, 102A>T (R34S) in exon 3, and 715G>A (G239S) in exon 8 (Fig. 1A,B). Studies of his family members demonstrated that his mother was heterozygous for 355C>T encoding Q119X, whereas his father and younger sister were heterozygous for 102A>T and 715G>T encoding R34S and G239S, respectively (Fig. 1A,B, data not shown). Q119X has been identified as one of the mutations for ADA-SCID (Ariga *et al*, 2001a), while G239S is a 'partial mutation' observed in a patient with partial ADA deficiency (Ariga *et al*, 2001b), There have been no reports of R34S mutation in ADA deficiency. To further determine whether the father's R34S and G239S mutations were both on the same allele, the reverse transcription polymerase chain reaction (RT-PCR) products consisting of full-length *ADA* cDNA were cloned and analysed for their nucleotide sequences. Only two clones were found: one with wild-type sequence and the other containing both R34S and G239S mutations. These results indicated that ADA-SCID in the patient was caused by compound heterozygous mutations: Q119X inherited from his mother and R34S/G239S from his father (Fig. 1B).

To study the effect of R34S/G239S mutations on ADA activity, the cDNAs containing the base changes individually and in combination were recloned into the pZ plasmid and introduced into the bacterial ADA-defective *E. coli* strain, SØ3834. ADA activity of each mutant cDNA expressed in SØ3834 was quantitated as previously described (Arredondo-Vega *et al*, 1998). Each R34S and G239S mutation resulted in 56·4% and 2·2% of normal ADA activity, respectively. However, the combination of R34S/G239S mutations resulted in 0·008% of normal ADA activity, indicating that the two mutations have synergistic effects on the loss of this activity (Fig. 1C).

Western blot analysis of the *E. coli* transformed with each mutant cDNA as previously described (Arredondo-Vega *et al*, 1998) revealed reduced expression of R34S or G239S mutant protein, whereas the combination of R34S/G239S resulted in no detectable protein expression (Fig. 1D). These results suggest that abolished ADA activity in R34S/G239S, is attributed to impaired protein expression. Direct sequence analysis of cDNA derived from his father demonstrated comparable signals of both wild-type and R34S/G239S mutant. In addition, sequence analysis of cloned RT-PCR products of *ADA* cDNA derived from his father showed wild-type and R34S/G239S mutant at a ratio of 7–5 (data not shown). These suggest that the lack of the mutant ADA protein expression is a result of protein instability, rather than mRNA instability.

doi:10.1111/j.1365-2141.2011.08640.x

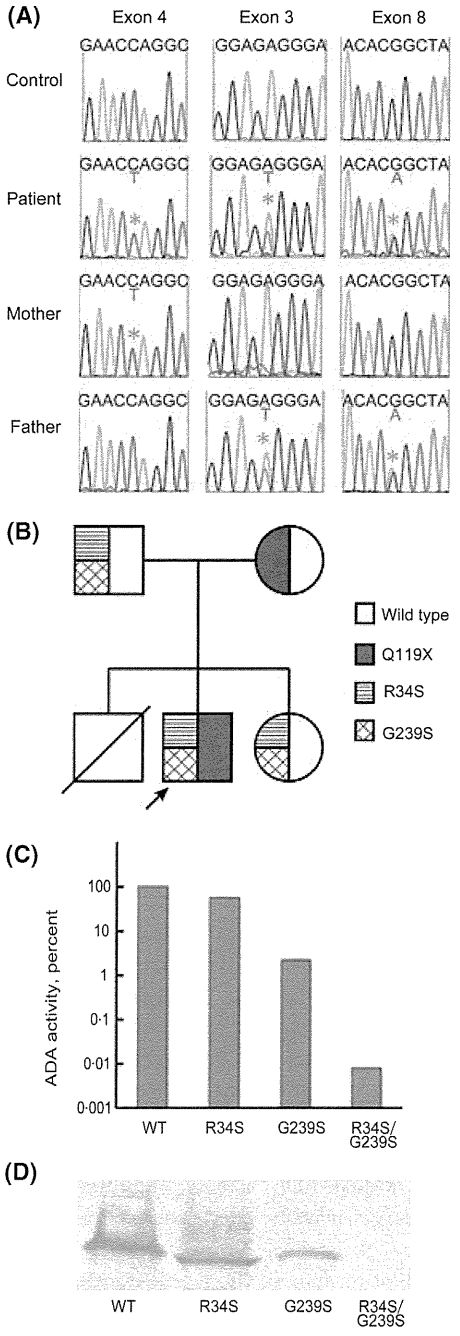

Fig 1. Studies of ADA sequence, activity, and expression. (A) Direct sequence analysis of the *ADA* gene in a control, the patient, mother, and father. The sites of mutations are indicated by asterisks. Left panels: Forward sequence of exon 4. 355C>T (Q119X) was present in the patient and his mother. Middle panels: Forward sequence of exon 3. 102A>T (R34S) was present in the patient and his father. Right panels: Forward sequence of exon 8. 715G>A (G239S) was present in the patient and his father. (B) Pedigree of the patient's family. Genotypes of the *ADA* are shown. An arrow indicates the patient. (C) ADA activity of mutants (R34S, G239S and R34S/G239S), expressed in *Escherichia coli*. Each mutant resulted in 56.4%, 2.2%, and 0.008% of the normal ADA activity, respectively. (D) Western blot analysis of ADA expression in lysates of SØ3834 in which wild-type, R34S, G239S, and R34S/G239S were expressed. R34S and G239S exhibited mildly and moderately reduced expression, respectively. R34S/G239S mutations in combination resulted in undetectable expression. WT, wild-type.

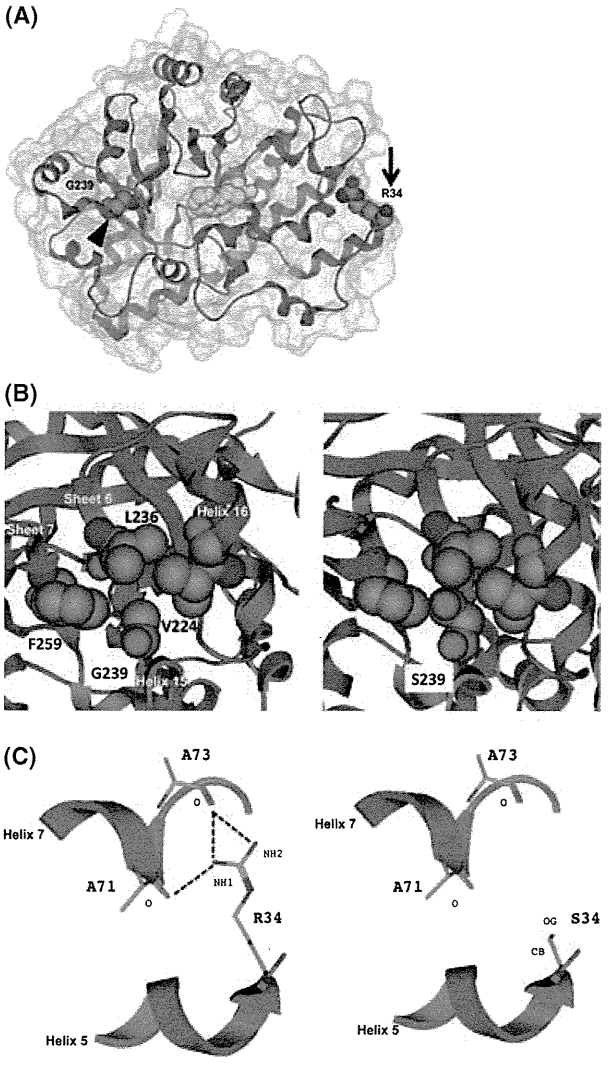

Fig 2. The effect of mutations on the tertiary structure of ADA. (A) Location of mutated residues, R34 and G239, are shown by an arrow and an arrowhead, respectively. The complexed ligand within the active site is represented by yellow spheres. (B) An enlarged view of regions neighbouring G239 (left) and S239 (right). Substitution of Gly to Ser, which has a hydrophilic side chain, weakens the hydrophobic force of the core. (C) An enlarged view of regions neighbouring R34 (left) and S34 (right). R34 is located in Helix 5. Substitution of Arg with Ser, which has a shorter side chain and lacks a positive charge, eliminates the hydrogen bonds, thereby affecting the ligand gating function of Helix 7. Hydrogen bonds are shown by dotted lines.

Next, we analysed the tertiary structure of the mutant ADA based on the crystal structure of human ADA (PDB code: 3IAR) as previously described (Montano *et al*, 2007) (Fig. 2A). G239 is a part of the hydrophobic core formed by Helices 15 and 16 and Sheets 6 and 7. Substitution of this amino acid with Ser, which has a hydrophilic side chain, retains the overall structure but weakens the hydrophobic force of the core (Fig. 2B). R34 is a positively charged peripheral residue located in Helix 5. Helix 5 forms hydrogen bonds with Helix 7, which is enables for the substrate to enter the active site. Substitution

of Arg with Ser, which has a shorter side chain and is uncharged, loses the hydrogen bonds. This causes a presumably unstable local structure, despite retained overall structure (Fig. 2C).

Jiang *et al* (1997) described the presence of two missense mutations on the same allele (L106V/Y97C), which synergistically abolished ADA activity independent of the protein instability. Therefore, the present report is the first to ADA-SCID in which two partial mutations on the same allele, R34S/G239S, synergistically abolished ADA protein stability. We named the combination of partial mutations that resulted in complete deficiency of the gene product 'WAZA-ARI' mutations, following a scoring system of Judo's competition. A 'waza-ari' is a half point; two 'waza-ari' scoring constitute the full point needed for win. In cases that lack correlation between genotype and phenotype, another mutation on the same allele should be assessed for 'WAZA-ARI' mutations.

Yuka Okura[1]
Masafumi Yamada[1]
Ichiro Kobayashi[1]
Ines Santisteban[2]
Gabriella Arredondo-Santisteban[2]
Zenichiro Kato[3]
Akihiro Iguchi[4]
Makoto Yoshida[4]
Osamu Ohara[5]
Noriko Nakagawa[6]
Kohsuke Imai[6]
Michael S. Hershfield[2]
Tadashi Ariga[1]

[1]Department of Paediatrics, Hokkaido University Graduate School of Medicine, Sapporo, Japan, [2]Departments of Medicine and Biochemistry, Duke University Medical Center, Durham, NC 27710, USA, [3]Department of Paediatrics, Gifu University Graduate School of Medicine, Gifu, Japan, [4]Department of Paediatrics, Asahikawa Medical College, Asahikawa, Japan, [5]Laboratory for Immunogenomics, Research Centre for Allergy and Immunology, RIKEN, Yokohama, Japan, and [6]Department of Paediatrics, National Defence Medical College, Tokorozawa, Japan
E-mail: tada-ari@med.hokudai.ac.jp

Acknowledgements

The authors thank the parents for their cooperation and all the physicians, nurses, and other personnel who participated in the care of the infant. We thank Drs Nobuaki Kawamura and Shunichiro Takezaki for critical discussion of the manuscript. This work was supported in part by a grant for Research on Intractable Diseases from the Japanese Ministry of Health, Labour and Welfare, and by Sigma-Tau Pharmaceuticals, Inc.

References

Ariga, T., Oda, N., Yamaguchi, K., Kawamura, N., Kikuta, H., Taniuchi, S., Kobayashi, Y., Terada, K., Ikeda, H., Hershfield, M.S., Kobayashi, K. & Sakiyama, Y. (2001a) T-cell lines from 2 patients with adenosine deaminase (ADA) deficiency showed the restoration of ADA activity resulted from the reversion of an inherited mutation. *Blood*, **97**, 2896–2899.

Ariga, T., Oda, N., Sanstisteban, I., Arredondo-Vega, F.X., Shioda, M., Ueno, H., Terada, K., Kobayashi, K., Hershfield, M.S. & Sakiyama, Y. (2001b) Molecular basis for paradoxical carriers of adenosine deaminase (ADA) deficiency that show extremely low levels of ADA activity in peripheral blood cells without immunodeficiency. *Journal of Immunology*, **166**, 1698–1702.

Arredondo-Vega, F.X., Santisteban, I., Daniels, S., Toutain, S. & Hershfield, M.S. (1998) Adenosine deaminase deficiency: genotype-phenotype correlations based on expressed activity of 29 mutant alleles. *American Journal of Human Genetics*, **63**, 1049–1059.

Daddona, P.E., Mitchell, B.S., Meuwissen, H.J., Davidson, B.L., Wilson, J.M. & Koller, C.A. (1983) Adenosine deaminase deficiency with normal immune function. An acidic enzyme mutation. *Journal of Clinical Investigation*, **72**, 483–492.

Hershfield, M.S. (2003) Genotype is an important determinant of phenotype in adenosine deaminase deficiency. *Current Opinion in Immunology*, **15**, 571–577.

Hershfield, M.S. & Mitchell, B.S. (2001) Immunodeficiency diseases caused by adenosine deaminase deficiency and purine nucleoside phosphorylase deficiency. In: *The Metabolic and Molecular Bases of Inherited Disease* (eds by C.R. Scriver, A.L. Beaudet, W.S. Sly & D. Valle) Vol 2, pp. 2585–2625, McGraw-Hill, New York.

Hirschhorn, R. & Ellenbogen, A. (1986) Genetic heterogeneity in adenosine deaminase (ADA) deficiency: five different mutations in five new patients with partial ADA deficiency. *American Journal of Human Genetics*, **38**, 13–25.

Jiang, C., Hong, R., Horowitz, S.D., Kong, X. & Hirschhorn, R. (1997) An adenosine deaminase (ADA) allele contains two newly identified deleterious mutations (Y97C and L106V) that interact to abolish enzyme activity. *Human Molecular Genetics*, **6**, 2271–2278.

Montano, A.M., Sukegawa, K., Kato, Z., Carrozzo, R., Di Natale, P., Christensen, E., Orii, K.O., Orii, T., Kondo, N. & Tomatsu, S. (2007) Effect of 'attenuated' mutations in mucopolysaccharidosis IVA on molecular phenotypes of N-acetylgalactosamine-6-sulfate sulfatase. *Journal of Inherited Metabolic Disease*, **30**, 758–767.

Morinishi, Y., Imai, K., Nakagawa, N., Sato, H., Horiuchi, K., Ohtsuka, Y., Kaneda, Y., Taga, T., Hisakawa, H., Miyaji, R., Endo, M., Oh-Ishi, T., Kamachi, Y., Akahane, K., Kobayashi, C., Tsuchida, M., Morio, T., Sasahara, Y., Kumaki, S., Ishigaki, K., Yoshida, M., Urabe, T., Kobayashi, N., Okimoto, Y., Reichenbach, J., Hashii, Y., Tsuji, Y., Kogawa, K., Yamaguchi, S., Kanegane, H., Miyawaki, T., Yamada, M., Ariga, T. & Nonoyama, S. (2009) Identification of severe combined immunodeficiency by T-cell receptor excision circles quantification using neonatal guthrie cards. *Journal of Pediatrics*, **155**, 829–833.

Mod Rheumatol
DOI 10.1007/s10165-011-0461-4

ORIGINAL ARTICLE

Enhanced exon 2 skipping caused by c.910G>A variant and alternative splicing of *MEFV* genes in two independent cases of familial Mediterranean fever

Yumi Tone · Tomoko Toma · Akiko Toga · Yasuhisa Sakakibara · Taizo Wada · Masahiro Yabe · Hiromitu Kusafuka · Akihiro Yachie

Received: 4 April 2011 / Accepted: 15 April 2011

Abstract Most reported cases of familial Mediterranean fever (FMF) involve missense mutations of *MEFV* concentrated within exon 10. We experienced two independent pedigrees of a unique variant in the *MEFV* gene that might cause excessive exon 2 skipping due to enhanced alternative splicing. In this study, we tried to elucidate the molecular mechanism of the *MEFV* variant as a cause of the FMF phenotype. Peripheral blood was obtained from volunteers and two patients with homozygous c.910G>A variant of the *MEFV* gene. *MEFV* messenger RNA (mRNA) expression patterns in mononuclear cells and granulocytes were compared using forward and reverse primers from exons 1 and 3, respectively. Expression profiles of pyrin were examined by transfecting wild-type and variant *MEFV* genes into HEK293T cells. Expression of normal-sized mRNA was extremely reduced in these patients, whereas that of aberrant short mRNA, deleting exon 2 (Δex2), was significantly increased. Immunohistochemical and immunoblotting analyses revealed a truncated immunoreactive pyrin protein in cells transfected with Δex2 cDNA. The *MEFV* gene c.910G>A variant results in accelerated aberrant splicing with abnormal protein size, presumably leading to anomalous pyrin function. This is the first report to show that an *MEFV* variant other than missense mutation is responsible for the FMF phenotype.

Keywords Familial Mediterranean fever · *MEFV* · Splice anomaly · Pyrin

Y. Tone · T. Toma · A. Toga · Y. Sakakibara · T. Wada · A. Yachie (✉)
Department of Pediatrics, School of Medicine, Institute of Medical, Pharmaceutical and Health Sciences, Kanazawa University, 13-1 Takaramachi, Kanazawa 920-8641, Japan
e-mail: yachie@staff.kanazawa-u.ac.jp

M. Yabe
Department of General Internal Medicine, Niigata City General Hospital, Niigata, Japan

H. Kusafuka
Department of General Internal Medicine, Nagoya Memorial Hospital, Nagoya, Japan

Introduction

Familial Mediterranean fever (FMF) is an autosomal recessive disease characterized by recurrent episodes of fever and serositis [1, 2]. Each episode of the attack continues for 1–4 days, and between attacks, symptoms can subside for several weeks to months. Left untreated, repeated episodes lead to AA amyloidosis and progression to renal failure. In some patients, unnecessary laparotomy is frequently performed due to recurrence of severe abdominal pain. Early diagnosis and appropriate therapeutic intervention is therefore mandatory to avoid these consequences. Although the vast majority of reported cases of FMF are from countries around the Mediterranean basin [3], as the name implies, patients from other part of the world are increasing in number [4, 5]. To date, more than 50 mutations in the FMF-associated gene (*MEFV*) have been identified in Japan since 1976 [6–8].

Mutations of the *MEFV* gene are concentrated within exon 10, and the major mutations—M694V, V726A, M694I, and M680I—comprise >74% of all reported mutations [3, 9, 10]. Notably, all of these mutations are missense, and no case has been reported with nonsense mutation or splice variants. In patients with FMF, pyrin dysfunction leads to aberrant molecular interactions

Published online: 12 May 2011

between these immunoregulatory proteins within inflammasome, resulting in the loss of regulatory function. The *MEFV* gene encodes pyrin, which is composed of five distinct domains. Among these domains, N-terminal PYRIN and C-terminal PRY-SPRY (B30.2) are thought to be responsible for major pyrin functions [11, 12]. PYRIN and PRY-SPRY associate with apoptosis speck protein (ASC) and caspase-1, respectively, and regulate the functions of inflammasome, leading to reduced levels of nuclear factor kappa-B (NF-κB) activation and interleukin-1β (IL-1β) production [13–16]. Among different *MEFV* mutations, the disease-related mutations within exon 10 have been the most thoroughly investigated to date. The functional interaction between the PRY-SPRY domain and caspase-1 appears to be inhibited in mutations involving M694 or M680, leading to excessive IL-1β production [17]. On the other hand, no mutation has been reported within the PYRIN domain, which has been shown to associate with ASC to control inflammation or to bind microtubules [17, 18].

In this report, we analyzed the molecular patterns of *MEFV* gene expression in two independent pedigrees of FMF patients who show a missense variant at the last nucleotide of exon 2. The patterns of mRNA expression and pyrin protein expression are shown for these cases.

Patients and methods

Patients

Patient 1 was a 61-year-old Japanese man who suffered from periodic episodes of fever and abdominal pain since the age of 43. The patient did not recall any episodes during his childhood. His abdominal pain was very severe and he had undergone repeated laparotomy under the diagnosis of appendicitis or cholelithiasis. No correct diagnosis was given for his suffering until his physician investigated the possibility of FMF. After we found the *MEFV* gene variant, he was started on colchicine. At the time of diagnosis, his serum C-reactive protein (CRP) was 6.3 mg/dl and white blood cell (WBC) count 3,200/μl. His symptoms resolved completely thereafter. No other person within his family showed similar symptoms.

Patient 2 was a 32-year-old Japanese woman with abdominal pain and lumbago. She was unrelated to patient 1, and her family history was unremarkable. Her lumbago developed at the age of 16. Since then, she experienced repeated episodes of severe abdominal pain of unknown origin and received laparotomy twice without any definitive diagnosis. Psychosomatic disease was the final diagnosis. She was treated with an antidepressant, without major improvement. She began having repeated febrile episodes 2 years prior to diagnosis, when FMF was suspected for the first time. At the time of diagnosis, her serum CRP was 0.1 mg/dl and WBC count 3,900/μl. An identical *MEFV* variant to that in patient 1 was found.

Gene analysis/sequence

Genomic DNA was isolated from peripheral leukocytes of the two patients and 125 healthy donors by standard procedures [19, 20]. We screened all *MEFV*-coding exons of DNA samples from patients and donors. Approval for the study was obtained from the Human Research Committee of Kanazawa University Graduate School of Medical Science, and informed consent from the two patients and all healthy donors was provided according to the Declaration of Helsinki.

MEFV mRNA/cDNA analysis

Peripheral blood mononuclear cells (PBMCs) were isolated by Ficoll–Hypaque gradient centrifugation from patients and normal controls [21]. Granulocytes were recovered from the pellet of the gradient after lysis of erythrocytes. Total RNA of granulocytes and monocytes were isolated by Trizol reagent (Invitrogen, Carlsbad, CA, USA). Complementary DNA (cDNA) was synthesized with the use of the oligo$(dT)_{20}$ primer and MMLV reverse transcriptase RNase H (ReverTra Ace, Toyobo Co., Ltd., Osaka, Japan) and amplified with GoTaq DNA polymerase using a forward primer located in exon 1 (5′-GTTCAAGCTGCAGAACACCAG-3′) and a reverse primer located in exon 3 (5′-AGTGTAAGCGCCAC CTGAAG-3′) of *MEFV*. The thermocycler conditions were as follows: one cycle of 5 min at 94°C followed by 40 cycles of 30 s at 95°C, 20 s at 60°C, and 30 s at 72°C, followed by final extension for 4 min at 72°C. The amplified products were separated by electrophoresis on a 1.5% agarose gel. The amplified fragments were detected by ethidium bromide staining of the agarose gel. Amplification of a fragment of the housekeeping gene β-actin was used as a positive control. Amount of amplified product was quantified by densitometry.

Activation of mononuclear cells by IFN-α or lipopolysaccharide (LPS)

PBMCs of patients and healthy controls were suspended in Roswell Park Memorial Institute (RPMI)-1640 containing 10% fetal calf serum (FCS) at 1×10^6/ml and stimulated with interferon alpha (IFN-α) (100 or 1,000 U/ml) or lipopolysaccharide (LPS) (10 or 100 ng/ml) for 8 h at 37°C in 5% carbon dioxide (CO_2). Total RNA was extracted from cultured cells, and *MEFV* mRNA expression was examined.

Plasmid construction and transfection for transient *MEFV* expression

The complete open reading frame of *MEFV* was amplified using specific primers (5′-CCGGAATTCGGCTAAGAC CCCTAGTGACCATCTG-3′ and 5′-ACGCGTCGACTG GGCATTCAGTCAGGCCCCTGACC-3′), and was subcloned into the pAcGFP1-C1 expression vector (Takara Bio, Otsu, Japan). To construct vectors carrying the G304R missense and the deleting exon 2 (Δex2) variants, the fragment of wild-type (WT) *MEFV* (exon 1–3) was replaced at the *Eco*RI and *Kpn*I sites with the variant sequences amplified from patient 1. All plasmid constructs were verified by sequencing. HEK293T cells were transfected with the vectors by lipofection using Lipofectamine™ 2000 (Invitrogen) and were harvested after 42-h culture at 37°C under 5% CO_2 [22].

Immunoblotting

Control HEK293T cells with mock plasmid (mock), WT *MEFV* gene, G304R single amino acid replacement (G304R) or pyrin with the exon 2 deletion (Δex2), or no transfectant were processed for immunoblotting with antipyrine antibody (R-13; Santa Cruz Biotechnology, Santa Cruz, CA, USA). Cell lysates were prepared with radioimmunoprecipitation assay (RIPA) lysis buffer (Santa Cruz) at 4×10^6/ml. Ku70 expression levels were determined simultaneously as internal controls with anti-Ku70 polyclonal antibody (M-19; Santa Cruz).

Immunofluorescence and immunohistochemistry

All cells were cultured in a Lab-Tek chamber slide (eight wells/slide, Nalge Nunc International, Naperville, IL, USA) for 48 h to obtain semiconfluent monolayers. After removing the medium chambers, slides were air-dried, fixed in acetone, and stored at −20°C until further analysis. Distribution of green fluorescent protein (GFP) was examined directly under a fluorescence microscope. Profiles of pyrin expression were examined by immunohistochemistry as described elsewhere using antipyrine antiserum [23].

Results

MEFV gene mutations

Figure 1 shows *MEFV* gene variants in our two cases. Homozygous c.910G>A variants were detected in DNA, which leads to the missense variants G304R. By screening 250 alleles from control donors, six alleles showed the identical variant. All of these control donors with *MEFV* variant were heterozygous carriers. According to National Center for Biotechnology Information Single Nucleotide Polymorphism (NCBI SNP) database, the frequency of c.910G>A variant is 1.4%, comparable with our analysis. No other mutation with amino acid substitution was found in either patient.

Increased Dex2 *MEFV* mRNA expression in patients of c.910G>A mutation

Reverse transcriptase polymerase chain reaction (RT-PCR) was performed using one set of primers spanning exon 2 of the *MEFV* gene (Fig. 2a). Although the short PCR products were seen in all six controls, the majority of products were 1,086-bp full-length products, with minimal short products. In marked contrast to the normal controls, most PCR products from the c.910G>A variant were short, with only trace levels of the full-length products (Fig. 2b). Calculation of the ratio of short to full-length products using densitometry data revealed significant differences between controls and patients (Fig. 2c). Both granulocytes and PBMCs from controls expressed five to ten times fewer short products than full-length products. In contrast, the ratio remained >2.5 in both granulocytes and PBMCs from the patients.

Short mRNA transcripts represent alternatively spliced *MEFV* mRNA

Full-length mRNA contained whole exon 2 with the G304R amino acid replacement (Fig. 3a). Direct gene

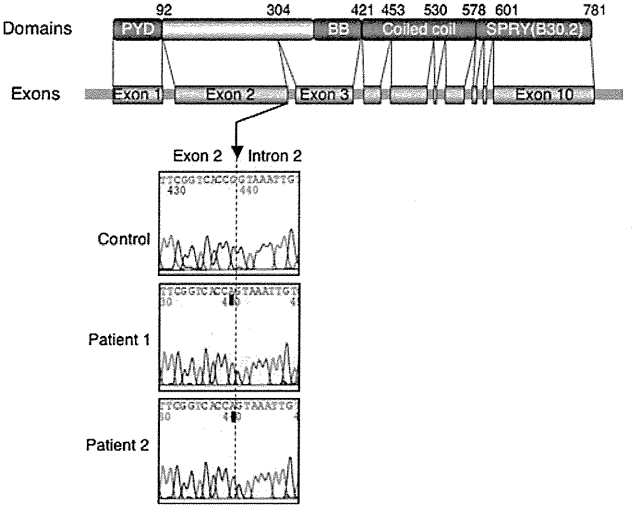

Fig. 1 *MEFV* gene structure and mutation analysis. Homozygous missense variant c.910G>A was found at the last nucleotide of exon 2 in patients 1 and 2. With normal splicing, this variant leads to a single amino acid replacement at the end of exon 2 (G304R)